

## Chapter 2

# Some Real(?) Problems in Earth Science

### 2.1 Introduction

Chapter 1 provided a basic recipe for concocting systems of conservation equations for just about any continuum problem you can imagine. This chapter will use this technique to set up a suite of fundamental physical problems that are important to many aspects of Earth science. The purpose of this chapter is not only derive the basic problems but to start to develop some basic physical intuition into how they behave. This intuition will be exceptionally important when we start to choose numerical methods that are appropriate for each problem. Nevertheless, when we are done, this chapter should demonstrate that despite the very different kinds of behaviour, as far as we are concerned numerically there are really only two kinds of problems; initial value problems (IVP's) that need to be marched carefully through time and boundary value problems (BVP's) that need to be satisfied simultaneously everywhere in space. Much interesting physics comes from combinations of these kinds of equations.

When you are done this course, should be able to solve all of the problems in this chapter as well as concoct your own custom problem. As for the basic problems in this chapter, these should be treated as the simplest examples of a class of problems and not taken for gospel. In general you should make up your own stories and build upon the framework of these problems (that's what theory is about). However, to be successful it is important to know the basic stories as well.

### 2.2 Thermal Convection

The first problem we will consider is that of thermal convection in fluids. Convection is simply the statement that hot fluids rise and cold fluids sink (more correctly low density fluids rise and high density fluids sink). Convection is a crucial process throughout the earth. Heating of the equator and cooling at the poles provides the basic engine for weather and climate change. The formation of cold

North-atlantic water contributes to the global *thermo-haline* circulation (which is technically *double-diffusive convection* because both heat and salt affect the densities.) Thermal convection in the mantle is the principal engine for plate tectonics and magneto-hydrodynamic convection in the core drives the Earth's dynamo and controls the Earth's magnetic field. Not too bad for a process where hot things rise and cold things sink. To gain some insight into convection, we will consider the simplest problem of thermal convection in a layer heated from below. This is the classic *Rayleigh-Benard* convection problem and is a favorite of physicists and earth-scientists everywhere.

### 2.2.1 Derivation

Starting with the general conservation equations for mass, momentum and heat for a viscous fluid, and assuming that the fluid is incompressible and has a constant viscosity then the *dimensional* governing equations for thermal convection can be written

$$\nabla \cdot \mathbf{V} = 0 \quad (2.2.1)$$

$$\frac{\partial T}{\partial t} + \mathbf{V} \cdot \nabla T = \kappa \nabla^2 T \quad (2.2.2)$$

$$\frac{\partial \mathbf{V}}{\partial t} + (\mathbf{V} \cdot \nabla) \mathbf{V} = \nu \nabla^2 \mathbf{V} - \frac{1}{\rho_0} \nabla P + \frac{\rho}{\rho_0} \mathbf{g} \quad (2.2.3)$$

Equation (2.2.1) is conservation of mass, (2.2.2) is conservation of heat and (2.2.3) is conservation of momentum. These equations have been written assuming a "Boussinesq Approximation" which says that the fluid densities are effectively constant  $\rho_0$  except in the body force terms where they drive most of the flow. For thermal convection the density of the fluid is temperature dependent

$$\rho = \rho_0(1 - \alpha(T - T_0)) \quad (2.2.4)$$

where  $\alpha$  is the *coefficient of thermal expansion*. In 2-D we can write out the  $x$  and  $z$  components of Eq. (2.2.3) as

$$\frac{\partial U}{\partial t} + \mathbf{V} \cdot \nabla U = \nu \nabla^2 U - \frac{1}{\rho_0} \frac{\partial P}{\partial x} \quad (2.2.5)$$

$$\frac{\partial W}{\partial t} + \mathbf{V} \cdot \nabla W = \nu \nabla^2 W - \frac{1}{\rho_0} \frac{\partial P}{\partial z} + (1 - \alpha(T - T_0))g \quad (2.2.6)$$

where we have substituted in (2.2.4). To make our lives easier (and this section much more confusing) it is useful to take the Curl of Eq. (2.2.3) to remove the gradient terms (remember  $\nabla \times \nabla f = 0$ ). If we also use  $\nabla \cdot \mathbf{V} = 0$  it can be shown that Eq. (2.2.3) becomes in 2-D

$$\frac{\partial \omega}{\partial t} + \mathbf{V} \cdot \nabla \omega = \nu \nabla^2 \omega - g\alpha \frac{\partial T}{\partial x} \quad (2.2.7)$$

where

$$\omega = (\nabla \times \mathbf{V}) \cdot \mathbf{k} = \left( \frac{\partial W}{\partial x} - \frac{\partial U}{\partial z} \right) \quad (2.2.8)$$

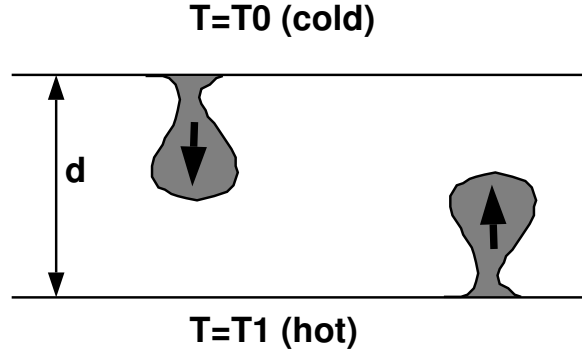


Figure 2.1: The geometry and physics of Rayleigh-Benard thermal convection. I.e. Hot goes up... cold goes down.

is the *vorticity*. Vorticity can be thought of as the local rate of rotation of a fluid particle. Comparison of Eqs. (2.2.2) and (2.2.7) shows that one is an advection-diffusion equation for Temperature, and the other is for vorticity, however the vorticity equation also has a source term  $g\alpha\partial T/\partial x$  i.e. lateral variations in temperature will drive rotational flow (i.e. convection). To finish the derivation we note that because the fluid is incompressible (Eq. 2.2.1) we can rewrite the velocity as

$$\mathbf{V} = \nabla \times \psi \mathbf{k} \quad (2.2.9)$$

where  $\psi$  is the *streamfunction*. This relationship is true because in general,  $\nabla \cdot (\nabla \times \mathbf{F}) = 0$  for all vectors  $\mathbf{F}$ .

Substituting into Eqs. (2.2.1)–(2.2.3) yields the dimensional 2-D equations in stream-function vorticity form

$$\frac{\partial T}{\partial t} + (\nabla \times \psi \mathbf{k}) \cdot \nabla T = \kappa \nabla^2 T \quad (2.2.10)$$

$$\frac{\partial \omega}{\partial t} + (\nabla \times \psi \mathbf{k}) \cdot \nabla \omega = \nu \nabla^2 \omega - g\alpha \frac{\partial T}{\partial x} \quad (2.2.11)$$

$$\nabla^2 \psi = -\omega \quad (2.2.12)$$

where Eq. (2.2.12) arises from the definitions of  $\psi$  and  $\omega$

## 2.2.2 Scaling

To determine the various magnitudes of each of the terms for the problem of a uniform layer of depth  $d$  with top temperature  $T_0$  and lower temperature  $T_1$  (see Fig. 2.1), it is now useful to scale everything to the thermal diffusive time scale, which is given by the time it takes for heat to diffuse across the layer. The typical scaling for this problem is

$$\begin{aligned} (x, z) &= d(x, z)' \\ t &= \frac{d^2}{\kappa} t' \end{aligned}$$

$$\begin{aligned}
\nabla &= \frac{1}{d} \nabla' & (2.2.13) \\
\mathbf{V} &= \frac{\kappa}{d} \mathbf{V}' \\
\omega &= \frac{\kappa}{d^2} \omega' \\
\psi &= \kappa \psi' \\
T &= T_0 + (T_1 - T_0) T'
\end{aligned}$$

Substituting and dropping primes yields the dimensionless equations

$$\frac{\partial T}{\partial t} + (\nabla \times \psi \mathbf{k}) \cdot \nabla T = \nabla^2 T \quad (2.2.14)$$

$$\frac{1}{\text{Pr}} \left( \frac{\partial \omega}{\partial t} + (\nabla \times \psi \mathbf{k}) \cdot \nabla \omega \right) = \nabla^2 \omega - \text{Ra} \frac{\partial T}{\partial x} \quad (2.2.15)$$

$$\nabla^2 \psi = -\omega \quad (2.2.16)$$

where  $\text{Pr} = \nu/\kappa$  is the *Prandtl Number* which is the ratio of momentum diffusivity to thermal diffusivity (i.e.  $\text{Pe}/\text{Re}$ ) and

$$\text{Ra} = \frac{\rho \alpha g \Delta T d^3}{\eta \kappa} \quad (2.2.17)$$

is the *Rayleigh Number* which measures the relative strength of buoyant time scale to the diffusive time scale.

For the Earth's mantle,  $\text{Pr} > 10^{24}$  so the inertial terms are completely negligible while  $\text{Ra} > 10^6$  so buoyancy forces are enormous. Thus when we are solving for mantle convection we usually assume the the Prandtl number is infinite and Eq. (2.2.15) reduces to

$$\nabla^2 \omega = \text{Ra} \frac{\partial T}{\partial x} \quad (2.2.18)$$

Note that the Peclet number seems to have disappeared from Eq. (2.2.14). It is actually there, however it has been defined to equal 1.

By all this jiggery pokery, we've turned 4 equations with 3 free parameters into 3 equations with one adjustable parameter. Note also that equations (2.2.18) and (2.2.16) have no time derivatives and must be satisfied everywhere instantaneously in space. These "Poisson equations" crop up in mathematical physics all the time. We will deal with their solution in gory detail later on.

### 2.2.3 Some solutions and a bit of physics

Figure 2.2 shows some numerical solutions for *infinite* Prandtl number Rayleigh-Benard convection in a 2 by 1 rectangular box. The beauty of RB convection is that, although there are three coupled equations for  $T$ ,  $\omega$  and  $\psi$ , there is only one adjustable parameter, the Rayleigh number  $\text{Ra}$ . Thus if we can do a suite of numerical runs (for the same boundary conditions) spanning  $\text{Ra}$  space we can map

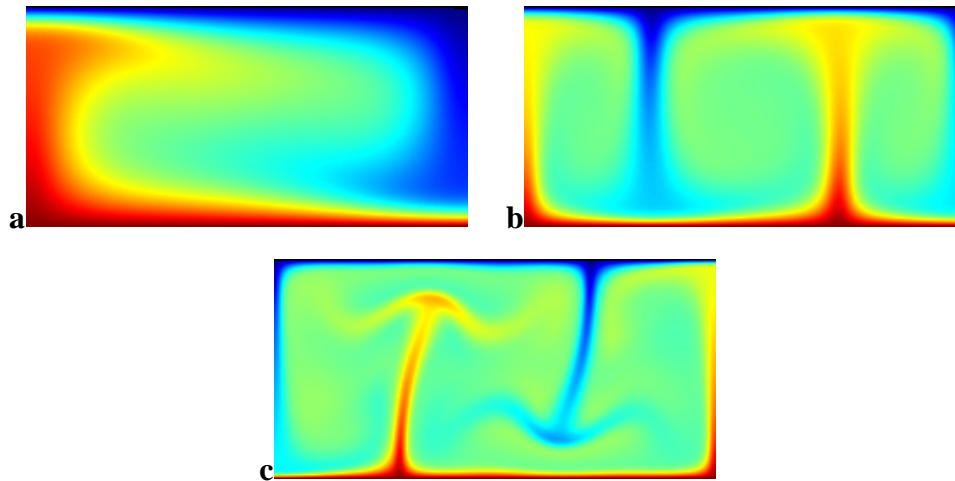


Figure 2.2: Some solutions for infinite Prandtl number Rayleigh Benard convection for different Rayleigh numbers. All of these solutions have free-stress boundary conditions with reflection sides for temperature. For numerical solution they use a combination of semi-Lagrangian and multi-grid techniques. (a)  $Ra = 10^4$ : convection goes to steady state with a broad symmetric upwelling and matching downwelling. (b)  $Ra = 10^5$ : upwellings and downwellings are narrower, more plentiful and become weakly time-dependent. (c)  $Ra = 10^6$ : convection becomes vigorous and time-dependent.

out the behaviour of these equations.<sup>1</sup> However, even with only one parameter the behaviour of these equations can be quite complex. Fortunately, there is an immense literature on this problem which lays out all the approximate and analytic (and numerical solutions) that can help you immensely in understanding new problems.

The most important feature of these equations is that there is a critical value of the Rayleigh number, below which no convection occurs. The actual value depends on the geometry of the box and the boundary conditions on temperature and flow. Below the critical  $Ra$  there is no motion and temperature is a vertical gradient. Right above the critical  $Ra$ , the problem usually forms a steady state set of convection rolls with equally spaced hot upwellings and cold downwellings (Fig. 2.2a). In 3-D these rolls can assume many interesting patterns (squares, hexagons, zig-zag rolls etc.). As  $Ra$  is increased, more energy is added to the system and the rolls begin to go time dependent. At very high  $Ra$  the system can go chaotic (Fig. 2.2c).

<sup>1</sup>this is a bit of a lie, actually. To solve these equations for a specific instance, you also have to impose boundary and initial conditions for the problem. As with most PDE's, changing the boundary conditions can drastically alter the behaviour of the problem.

### 2.2.4 Another approach to convection: the Lorenz Equations and chaos

Another version of the Rayleigh-Benard convection problem also features prominently in the story of chaos (see Gleick [1] for a good read) as it is the foundation for the most famous of chaotic problems *The Lorenz Equations*. As discussed, rather elegantly, by Edward Lorenz [2], the Lorenz equations are a simplified toy model of Raleigh-Bernard convection that were developed to demonstrate the unpredictability of chaotic systems. They also form a good example of another important class of problems that need numerical solutions and that is systems of non-linear ordinary differential equations (or non-linear dynamical systems).

The Lorenz Equations are simplifications of the full PDE's Eqs. (2.2.14)–(2.2.16) that assume that the spatial structure of the velocity and temperature field are known and only solve for the time-dependent amplitudes. More specifically he assumed he could write  $\psi$  and  $T$  as a truncated 2-D Fourier series as

$$\psi = W(t) \sin(\pi ax) \sin(\pi z) \quad (2.2.19)$$

$$T = (1 - z) + T_1(t) \cos(\pi ax) \sin(\pi z) + T_2(t) \sin(2\pi z) \quad (2.2.20)$$

which assumes that the velocity field can be described by a pair of counter-rotating rolls with a wavelength of  $2/a$  and that the temperature can be described as the sum of three modes. The first is a steady state ramp that is hot on the bottom and cold on the top, the second mode controls horizontal temperature gradients and the third mode controls vertical temperature gradients. Since the spatial variation is assumed known, the only unknowns are the time-dependent coefficients  $W$ ,  $T_1$ ,  $T_2$ . Substituting Eqs. (2.2.19) and (2.2.20) into Eqs. (2.2.14)–(2.2.16) and collecting terms with common modes yields a system of non-linear ordinary differential equations for the time dependent coefficients.

$$\begin{aligned} \frac{dW}{dt} &= \text{Pr}(T_1 - W) \\ \frac{dT_1}{dt} &= -WT_2 + rW - T_1 \\ \frac{dT_2}{dt} &= WT_1 - bT_2 \end{aligned} \quad (2.2.21)$$

where  $r$  is the value of the Raleigh number normalized by the critical Rayleigh number ( $\text{Ra}/\text{Ra}_c$ ) and  $b = 4/(1 + a^2)$ . Equation (2.2.21) is a good example of a *spectral method* where the solution is expanded in terms of Fourier modes; however, in this case the expansion is severely truncated to just the first few modes.

For  $r$  close to 1, the solution of the Lorenz equations is a good approximation to that of the full equations. At high values of  $r$ , however, it is not because it does not have enough degrees of freedom to generate new convection cells. Nevertheless, this system of equations does show remarkable aperiodic behaviour in that the direction the convection roll turns flips in a chaotic fashion. Figure 2.3 shows the time-series for the classic solution of the equations with  $r = 28$ ,  $\text{Pr} = 10$  and  $b = 8/3$ .

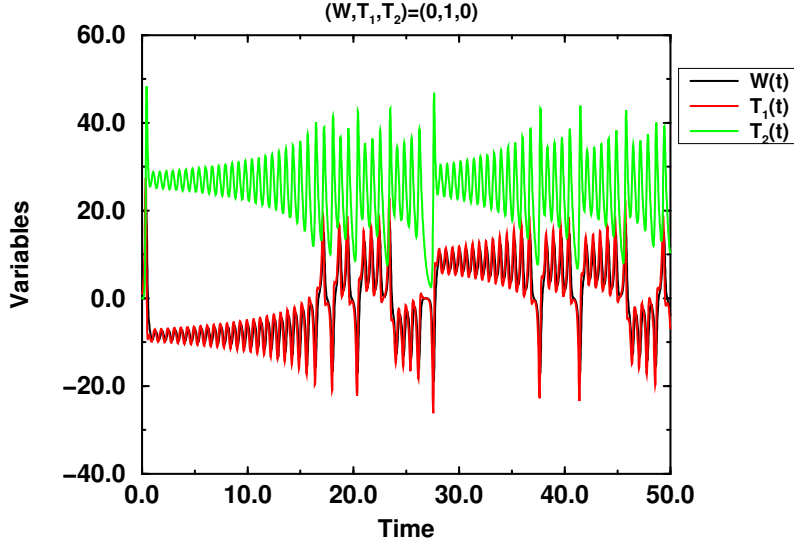


Figure 2.3: Time series of  $W$ ,  $T_1$  and  $T_2$  for the Lorenz equations with  $r = 28$ ,  $Pr = 10$  and  $b = 8/3$ . Positive  $W$  means clockwise rotation, Negative  $W$  means counter-clockwise rotation. Note the erratic flipping with growing oscillations that is characteristic of these chaotic equations.

### 2.3 Shallow water equations

Convection governs vertical motions of fluids in the earth; however, for many problems such as large-scale ocean and atmosphere dynamics, the scale of horizontal motions is much larger than the scale of vertical motions. Thus it is often convenient to consider an approximate version of the equations of motions in a rotating frame Eq. (1.3.9) where we assume that the fluid is confined to layer which is much thinner than it is wide. We also assume that vertical motions only change the layer depth and that the pressure gradient is near hydrostatic. A full derivation of the shallow water equations and a discussion of where they are valid can be found in any good ocean-atmosphere text such as Gill [3].

The shallow-water equations for flow of fluid on a rotating sphere (aka the Earth) in spherical polar coordinates were derived by Laplace to be

$$\frac{Du}{Dt} - \left(2\Omega + \frac{u}{r \cos \phi}\right) v \sin \phi = -\frac{g}{r \cos \phi} \frac{\partial \eta}{\partial \lambda} \quad (2.3.1)$$

$$\frac{Dv}{Dt} + \left(2\Omega + \frac{u}{r \cos \phi}\right) u \sin \phi = -\frac{g}{r} \frac{\partial \eta}{\partial \phi} \quad (2.3.2)$$

$$\frac{\partial \eta}{\partial t} + \frac{1}{r \cos \phi} \left\{ \frac{\partial}{\partial \lambda} [(H + \eta)u] + \frac{\partial}{\partial \phi} [(H + \eta)v] \right\} = 0 \quad (2.3.3)$$

where  $\lambda$  is the longitude and  $\phi$  is the latitude.  $u$  is the horizontal velocity in the longitudinal direction or zonal flow ( $u > 0$  is eastward flow),  $v$  is meridional flow ( $v > 0$  is northward flow). Note, the material derivative  $D/Dt$  only applies to horizontal motion. Vertical motion is neglected in these equations except for how

it affects  $\eta$ , the perturbed thickness of the water layer which has an equilibrium depth of  $H$  in the absence of any motion.  $\Omega$  is the Coriolis rotational velocity and  $r$  is the radius of the sphere. These equations look rather complicated but most of that is due to the interactions of the spherical geometry and the Coriolis terms (and this is what makes ocean-atmosphere dynamics interesting). The basic physics is straightforward however. Variations in layer thickness  $\eta$  drive horizontal fluid motions which are modified by the Coriolis forces which make the velocities turn. The divergence or convergence of the horizontal velocities, however, change the layer thickness and the three variables feed-back on each other and propagate as waves. While it is not obvious from the form of Equations (2.3.1)–(2.3.3), these equations are effectively a complicated wave-equation for how a thin inviscid layer tries to adjust to equilibrium.

### 2.3.1 Linearized Shallow water equations for the equatorial $\beta$ plane

Unless you're interested in planetary scale flow, Eqs. (2.3.1)–(2.3.3) are a bit of overkill<sup>2</sup> and additional simplifications can be made for specific regions of the planet. An important region for the evolution of climate is the tropics and a useful approximation of the full spherical equations near the equator can be made using the *Equatorial Beta plane* approximation. Near the equator,  $\phi$  is small so  $\sin \phi \approx \phi$  and  $\cos \phi \approx 1$ . Moreover we can project our spatial positions onto a plane tangent to the equator such that our new east-west coordinate is  $x = r\lambda$  and our north-south coordinate is  $y = r\phi$ . The Coriolis parameter  $f$  is defined as  $f = 2\Omega \sin \phi$ . If we also define the beta parameter as

$$\beta = \frac{1}{r} \frac{df}{d\phi} = \frac{2\Omega \cos \phi}{r} \quad (2.3.4)$$

the Coriolis parameter becomes  $f = \beta y$  near the equator.

Substituting these relationships into Eqs. (2.3.1)–(2.3.3) and assuming that the overall velocities are sufficiently small that products of velocities are much smaller than the velocity themselves (i.e.  $u^2, v^2, uv \ll u, v$ ) then the linearized shallow-water equations on the equatorial beta plane can be written

$$\frac{\partial u}{\partial t} - \beta y v = -g \frac{\partial \eta}{\partial x} \quad (2.3.5)$$

$$\frac{\partial v}{\partial t} + \beta y u = -g \frac{\partial \eta}{\partial y} \quad (2.3.6)$$

$$\frac{\partial \eta}{\partial t} + \frac{\partial(Hu)}{\partial x} + \frac{\partial(Hv)}{\partial y} = 0 \quad (2.3.7)$$

These equations admit a large number of analytic wave solutions and are discussed in detail in Gill [3]. The most important feature of these equations is that the Coriolis force vanishes on the equator  $y = 0$  yet increases in both directions away from it. These features of the beta plane cause wave energy to be trapped near the

---

<sup>2</sup>an interesting application of them however is for the development of atmospheric patterns in the atmosphere of Jupiter by Lorenzo Polvani [4]

equator, i.e. the equator acts as a wave guide. In particular there are two important kinds of waves that arise in the tropics that are of interest in climate studies. The fastest moving waves are the eastward propagating *Kelvin Waves*, that have no north-south component of velocity and move at a constant velocity, independent of the east-west wavenumber. Typical Kelvin waves for the Pacific might move about  $3 \text{ ms}^{-1}$  and take about 2 months to cross the Pacific. The other important waves are the equatorial *Rossby waves* or *planetary waves*. These are more slowly moving (the fastest Rossby wave is about a third the speed of the Kelvin wave) and have phase velocities that propagate westward. It is generation of Kelvin and Rossby waves by the atmosphere that gives rise to the Pacific climate oscillation known as El Niño.

### 2.3.2 El Niño prediction the Cane/Zebiak way

Equations (2.3.5)–(2.3.7) play a fundamental role in the Cane-Zebiak model of El Niño forecasting (e.g. [5–7]). This model is a simplified, coupled ocean-atmosphere model where the ocean is described by the forced equatorial shallow water equations (plus a little bit). Qualitatively, the tropical dynamics in this model is that variations in sea-surface temperature drive winds in the atmosphere. These winds then drive the ocean which generates Kelvin and Rossby waves which transport the sea-surface temperature field and so on. The principal additions to Eqs. (2.3.5)–(2.3.7) are the forcing by the wind stress vector  $\tau = (\tau_x, \tau_y)$  and an appropriate damping term to dissipate the forced energy. The model also assumes a constant undisturbed layer depth  $H_0$ . With these assumptions, the dimensional ocean model for Cane-Zebiak can be written.

$$\frac{\partial u}{\partial t} - \beta y v = -g H_0 \frac{\partial \eta}{\partial x} + \tau_x / \rho - r u \quad (2.3.8)$$

$$\frac{\partial v}{\partial t} + \beta y u = -g H_0 \frac{\partial \eta}{\partial y} + \tau_y / \rho - r v \quad (2.3.9)$$

$$\frac{\partial \eta}{\partial t} + \frac{\partial u}{\partial x} + \frac{\partial v}{\partial y} + r \eta = 0 \quad (2.3.10)$$

The dissipation terms,  $-r\mathbf{v}$ ,  $-r\eta$  are simplistic *Rayleigh Friction* terms that act exactly the same way radioactive decay works. Without this term, the energy in the ocean model would just keep increasing with time which is unrealistic. In addition to the bulk ocean transport, the model also includes a surface *frictional layer* that mimics local ocean upwelling due to surface wind divergence. Variations in the oceanic upwelling also affects the sea surface temperature by bringing up (or pushing down) colder water at depth. The remarkable thing about this model is its simplicity. It is not a fully non-linear coupled ocean-atmosphere model with thermodynamics and the kitchen sink. It is actually a very graceful simplified notion of the interaction of the ocean and atmosphere in the tropical Pacific that captures the essential physics with the minimal effort and is actually useful for predicting climate changes (sometimes). That's the hallmark of an excellent model and a style you should strive for.

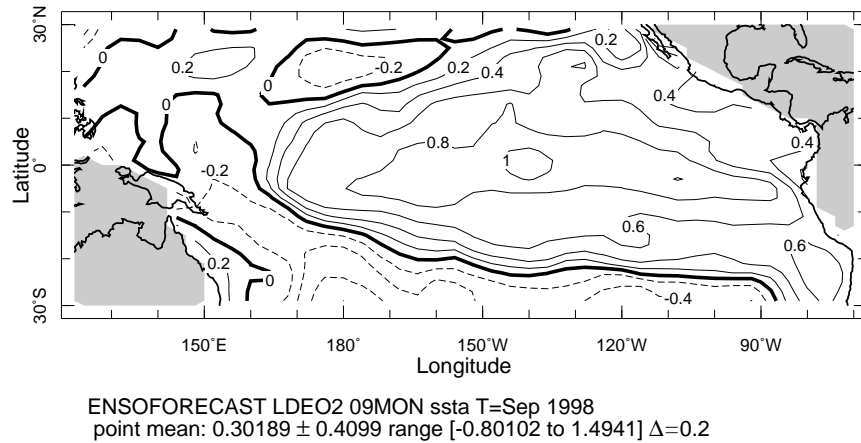


Figure 2.4: Picture of the predicted Sea Surface Temperature anomaly (SSTA) from the current LDEO2 model of El Niño. Predictions are for September 1998. Model domain does not include the grey areas. The basic physics of this model is that variations in the sea-surface temperature drive winds in the atmosphere (which is also governed by a set of shallow “water” equations). These winds, induce wave motions in the oceans and the currents associated with the waves transport the sea-surface temperatures. These models formed the basis for forecasting used by the IRI, although currently a larger range of models are used. For more information see <http://iri.columbia.edu/>

## 2.4 Seismic Wave propagation

The ocean and atmosphere are an endless source of wave propagation problems. The other classic source, of course, is in seismology where 90% of what we know about the structure and properties of the solid earth deeper than a few kilometers comes from understanding the behaviour of seismic waves. Much like a full solution of the Navier stokes equation for the ocean and atmosphere is currently untractable, so is a full solution of the wave equation for the interior of the earth (although, newer models running on the worlds fastest supercomputers are beginning to challenge this statement). For most problems, there are a number of extremely useful approximate schemes that actually allow us to do sophisticated problems without actually solving the full wave equation numerically. Nevertheless, there are times when the approximate theory is not enough or the geometry of the seismic velocity fields are too complicated that it is necessary to actually brute force it. Times when numerical solutions are useful include doing time migration in exploration seismics, analyzing the interaction between seismic waves and geologic structures or simply desiring to make pretty pictures. The techniques themselves are not particularly difficult, the challenge is to model efficiently. The following discussion is heavily cribbed from a very useful set of notes by Gustavo Correa, LDEO.

### 2.4.1 Basic derivation: linear elastic media

The general equations for conservation of momentum for a deformable continuum is given by Eq. (1.2.7) as

$$\rho \frac{D\mathbf{V}}{Dt} = \nabla \cdot \boldsymbol{\sigma} + \rho \mathbf{g} + \mathbf{f} \quad (2.4.1)$$

where  $\mathbf{f}$  are any other transient forces (explosions, earthquake sources) in addition to gravity. For the case of wave propagation in an elastic material we can assume that the overall displacements will be small such that

$$\frac{D\mathbf{V}}{Dt} \approx \frac{\partial \mathbf{V}}{\partial t} \quad (2.4.2)$$

and that the stress tensor for an isotropic, linearly elastic solid can be written in component form as

$$\sigma_{ij} = 2\mu\epsilon_{ij} + \lambda\epsilon_{kk}\delta_{ij} \quad (2.4.3)$$

where  $\mu$  is the *shear modulus*,  $\lambda$  is the *bulk modulus* and the strain tensor is

$$\epsilon_{ij} = \frac{1}{2} \left( \frac{\partial u_i}{\partial x_j} + \frac{\partial u_j}{\partial x_i} \right) \quad (2.4.4)$$

and  $\mathbf{u}$  is the local displacement vector. Furthermore, we will assume that both the stress tensor and the total displacement can be decomposed into a static component that balances the loading by body forces (the *pre-stressed displacements*) and a transient component that is important during elastic wave propagation. i.e.

$$\mathbf{u}_{tot} = \mathbf{u}_0 + \mathbf{u} \quad (2.4.5)$$

$$\boldsymbol{\sigma}_{tot} = \boldsymbol{\sigma}_0 + \boldsymbol{\sigma} \quad (2.4.6)$$

where  $\mathbf{u}_0$  are the solutions of the static problem

$$\nabla \cdot \boldsymbol{\sigma}_0 + \rho \mathbf{g} = 0 \quad (2.4.7)$$

Taking the time derivatives of (2.4.5) and (2.4.6) and substituting in Eqs. (2.4.1), (2.4.3) and (2.4.4) yields the equations for wave propagation

$$\rho \frac{\partial \mathbf{V}}{\partial t} = \nabla \cdot \boldsymbol{\sigma} + \mathbf{f} \quad (2.4.8)$$

$$\frac{\partial \sigma_{ij}}{\partial t} = \mu \left( \frac{\partial V_i}{\partial x_j} + \frac{\partial V_j}{\partial x_i} \right) + \lambda \nabla \cdot \mathbf{V} \delta_{ij} \quad (2.4.9)$$

which in 3-D is 9 coupled first order PDE's for the three displacements and six independent components of the stress tensor (don't forget  $\boldsymbol{\sigma}$  is symmetric such that  $\sigma_{ij} = \sigma_{ji}$ ). These equations form the basis for the most common forms of solution of the elastic wave equations.

It is also possible to use this approach to solve for *acoustic waves* in a material that cannot support shear (i.e. fluids with  $\mu = 0$ ). In this case stress is just given by a scalar pressure

$$\sigma_{i,j} = -P\delta_{ij} \quad (2.4.10)$$

If we also define the *dilation rate*  $\mathcal{D} = \nabla \cdot \mathbf{V}$  as the rate of expansion (or contraction) then by substituting (2.4.10) into (2.4.8) and taking the divergence of this equation we get.

$$\frac{\partial \mathcal{D}}{\partial t} = -\nabla \cdot \frac{1}{\rho} \nabla P + \nabla \cdot \frac{\mathbf{f}}{\rho} \quad (2.4.11)$$

and Eq. (2.4.9) becomes

$$\frac{\partial P}{\partial t} = -\lambda \mathcal{D} \quad (2.4.12)$$

Alternatively, we can combine Eqs. (2.4.11) and (2.4.12) into a single second order equation for the pressure (or dilation rate)

$$\frac{1}{\rho c^2} \frac{\partial^2 P}{\partial t^2} = \nabla \cdot \frac{1}{\rho} \nabla P - \nabla \cdot \frac{\mathbf{f}}{\rho} \quad (2.4.13)$$

where  $c = \sqrt{\lambda/\rho}$  is the acoustic wave speed.

Figure 2.5 shows the behaviour of the pressure field for a calculation that uses a *pseudo-spectral* technique to model the behaviour of a seismic pulse in a layered sedimentary basin with salt in it (Correa, pers. comm). We will visit the numerical tricks and traps of this problem later but suffice it to say that the real difficult part of this problem is implementing useful boundary conditions. However, given the model, synthetic seismograms and record sections can be constructed that can be compared with data to understand what features are diagnostic (Fig. 2.6)

## 2.5 Flow in porous media

We've done fluids... We've done solids... now it's time to talk about that murky region where fluids and solids interact. In the Earth there are a large number of problems that can be described by the interaction of a low viscosity fluid (water, oil, gas, magma) in a permeable (and possibly deformable) matrix. First we will discuss the classic equations for flow in rigid porous media. Then section 2.5.2 will develop the equations for flow in deformable porous media, in the context of the the most drastic of these problems, magma migration from the convecting mantle. Finally we show that all the standard problems of flow in rigid or elastic media (hydrology, fluid flow in sedimentary basins) can be derived from this more general framework.

### 2.5.1 Rigid porous media

*Darcy's Law* is the classic, empirically derived equation for the flux  $\mathbf{q}$  of a low viscosity fluid in a permeable matrix and can be written

$$\mathbf{q} = \frac{k_\phi}{\mu} [\nabla P - \rho_f \mathbf{g}] \quad (2.5.1)$$

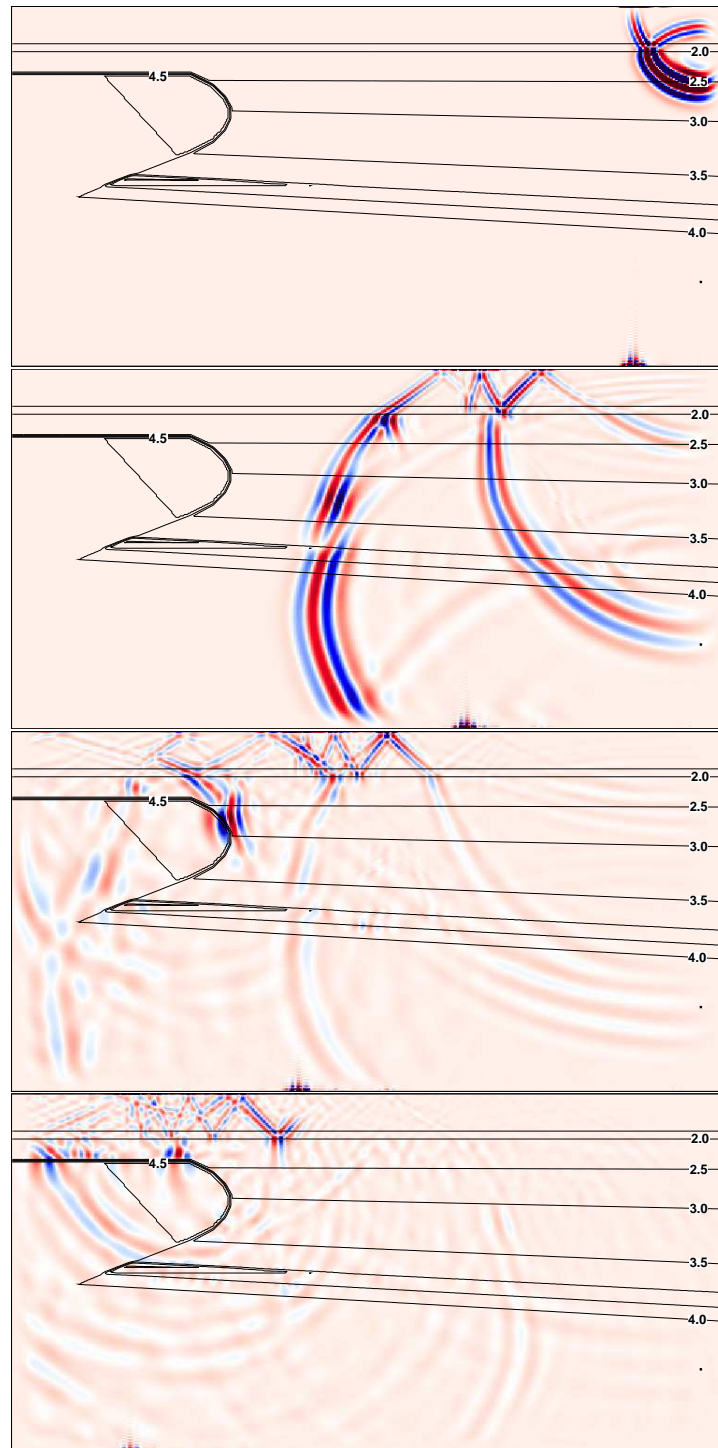


Figure 2.5: Evolution of pressure from a single shot in a layered sedimentary basin overlain by water. Time increases from top to bottom. High pressure regions are red, low pressure regions are blue and lines show P-wave velocity structure. The high velocity blob to the left is a region of salt, the top layer is water. This calculation was done by Gustavo Correa using a pseudo-spectral technique which is highly accurate for wave problems.

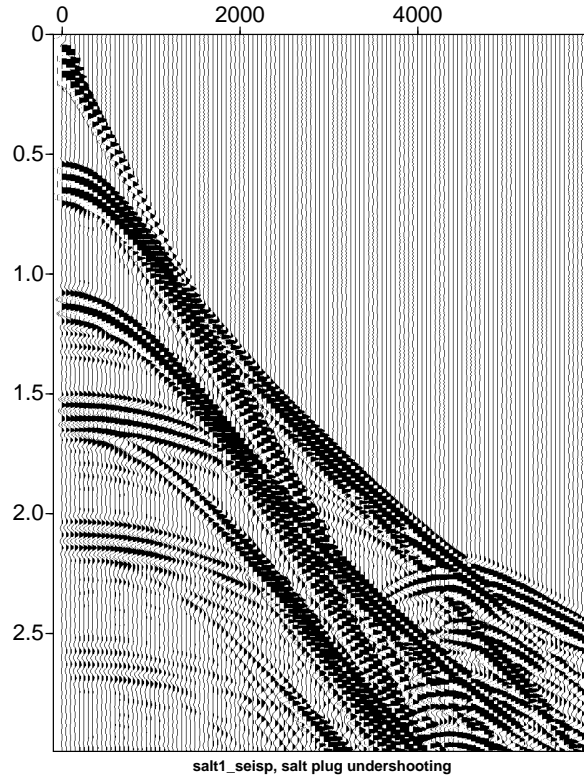


Figure 2.6: Synthetic shot gather from calculation show in Figure 2.5. Again this calculation was done by Gustavo Correa at LDEO.

where  $k_\phi$  is the macroscopic permeability of the medium (and can be a tensor),  $\mu$  is fluid viscosity,  $P$  is the fluid pressure and  $\rho_f$  is the fluid density. This equation assumes that flow in the pores or cracks of the medium is essentially laminar and provides the *average* flux through a representative area that is larger than the pore scale and smaller than the scale of significant permeability variation (if such a scale exists). Various approaches have been used to justify this rule from first principles (e.g. see Dagan [8]) but it generally seems to work. At any rate the principal unknown in all of these problems is the proper functional form for the permeability which can vary by orders of magnitude over relatively small distances. Much of hydrology and reservoir modeling is concerned with coming up with reasonable permeability structures.

One way to solve these equations however is to note that, in a rigid medium, if the fluid is incompressible and there is no significant mass transfer between solid and liquid, then

$$\nabla \cdot \mathbf{q} = 0 \quad (2.5.2)$$

because whatever fluid enters a volume must come out. Substituting in Eq. (2.5.1) and rearranging yields a modified Poisson problem for the fluid pressure

$$\nabla \cdot \frac{k_\phi}{\mu} \nabla P = \nabla \cdot \frac{k_\phi \rho \mathbf{g}}{\mu} \quad (2.5.3)$$

which says that the fluid pressure gradient must adjust to balance the buoyancy forces driven by gravity. This equation is another boundary value problem, much like the standard Poisson problems we saw in Section 2.2. However, because the permeabilities are not, in general, constant, many of the rapid methods that can be used for solving  $\nabla^2\Phi = f$  cannot be used. However, iterative *multigrid* methods (Chapter 9) can often be used with equal efficiency on either kind of problem. Figure 2.7 shows the 2-D flow field through a rigid and slightly elastic porous media with heterogeneous permeability.

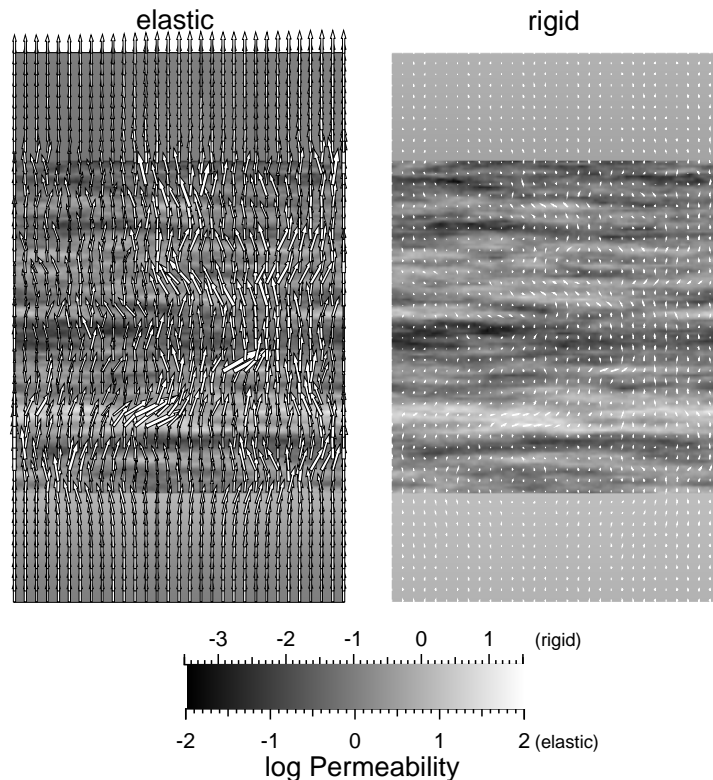


Figure 2.7: Flow field through a heterogeneous porous medium.

### 2.5.2 Deformable porous media: magma migration

Flow in rigid and elastic media is useful for problems in hydrology and crustal fluid flow. However, the melting and motion of partially molten rocks is a fundamental feature of plate tectonics and controls the geochemical evolution of the planet. To understand the behaviour of partially molten rock in the mantle (e.g. for regions beneath mid-ocean ridges, subduction zones and mantle plumes) requires a theory that has, at the very minimum, four important properties. The system needs at least two phases (solid and liquid), there must be significant mass-transfer between the solid and liquid (i.e. melting and freezing), the solid must be permeable at some scale, and the solid in the mantle must be viscously deformable so that, in

the absence of melting the theory is consistent with mantle convection (Section 2.2). Given these basic assumptions and a will to succeed, McKenzie [9] and others [10–12] derived a system of conservation equations for a two-phase mixture of a low viscosity liquid in a viscously deformable porous medium. McKenzie [9] provides a particularly detailed derivation that uses many of the concepts in Chapter 1. The general, dimensional equations for conservation of mass and momentum look like

$$\frac{\partial(\rho_f \phi)}{\partial t} + \nabla \cdot (\rho_f \phi \mathbf{v}) = \Gamma \quad (2.5.4)$$

$$\frac{\partial[\rho_s(1 - \phi)]}{\partial t} + \nabla \cdot [\rho_s(1 - \phi)\mathbf{V}] = -\Gamma \quad (2.5.5)$$

$$\phi(\mathbf{v} - \mathbf{V}) = \frac{-k_\phi}{\mu} [\nabla P - \rho_f \mathbf{g}] \quad (2.5.6)$$

$$\nabla P = -\nabla \times [\eta \nabla \times \mathbf{V}] + \nabla [(\zeta + 4\eta/3)\nabla \cdot \mathbf{V}] + \mathbf{G} - \bar{\rho} \mathbf{g} \quad (2.5.7)$$

$$k_\phi \sim \frac{a^2 \phi^n}{b} \quad (2.5.8)$$

Where  $\rho_f$ ,  $\rho_s$  are the melt and solid densities,  $\phi$  is the volume fraction of melt (porosity),  $\mathbf{v}$  and  $\mathbf{V}$  are the melt and solid velocities and  $\Gamma$  is the total rate of mass transfer from solid to liquid.  $k_\phi$  is the permeability which is a non-linear function of porosity (Eq. 2.5.8),  $\mu$  is the melt viscosity,  $P$  is the fluid pressure and  $\mathbf{g}$  is the acceleration due to gravity. Finally,  $\eta$  is the solid shear viscosity,  $(\zeta + 4\eta/3)$  is the combination of solid bulk and shear viscosity that controls volumes changes of the matrix,  $\mathbf{G}(\eta, \mathbf{V})$  are the cross-terms that arise for non-constant shear viscosity (and vanish if  $\eta$  is constant) and  $\bar{\rho} = \rho_f \phi + \rho_s(1 - \phi)$  is the mean density of the two phase system. Equations (2.5.4) and (2.5.5) conserve mass for the melt and solid respectively and allow mass-transfer between the phases. Equation (2.5.6) governs the separation between melt and solid and Eq. (2.5.7) governs stress-balance and deformation of the solid phase.

So far, this is the ugliest set of equations we've had to deal with yet but it's surprising what a bit of analysis (and ten years of banging your head against a wall) can do to bring out the behaviour in what was essentially a new problem in Earth science. The first trick was to realize that Eqs. (2.5.4)–(2.5.8) can be rewritten in a more tractable form that highlights the essential physics. All the detail can be found in Spiegelman [13, 14].

### Equations in potential form

The key feature of these equations is that the solid phase can deform in two fundamentally different ways. It can shear and convect like the standard incompressible convection equations; however, it can also compact or expand to expel (or inflate with) melt. One way to explicitly separate these two kinds of behaviour is to use *Helmholtz' Theorem* that says that any vector field can be decomposed into a incompressible and a compressible part, i.e.

$$\mathbf{V} = \nabla \times \Psi^s + \nabla \mathbf{u} \quad (2.5.9)$$

where  $\Psi^s$  is the stream-function as before and  $\mathbf{u}$  is a scalar potential field. Remembering the basic vector calculus identities that  $\nabla \cdot (\nabla \times \mathbf{F}) \equiv 0$  and  $\nabla \times (\nabla \mathbf{F}) \equiv 0$  shows that the first term is incompressible and the second term is irrotational. Using these definitions and also defining the *compaction rate*

$$\mathcal{C} = \nabla \cdot \mathbf{V} \quad (2.5.10)$$

and substituting into the 2-D equations with constant viscosities and densities yields the governing equations in *potential form*

$$\frac{\partial \phi}{\partial t} + \mathbf{V} \cdot \nabla \phi = (1 - \phi)\mathcal{C} + \frac{\Gamma}{\rho_s} \quad (2.5.11)$$

$$-\nabla \cdot \frac{k_\phi}{\mu} (\zeta + 4\eta/3) \nabla \mathcal{C} + \mathcal{C} = \nabla \cdot \frac{k_\phi}{\mu} \left[ \eta \nabla \times \nabla^2 \psi^s \mathbf{j} - (1 - \phi) \Delta \rho g \mathbf{k} \right] + \Gamma \quad (2.5.12)$$

$$\nabla^2 \mathcal{U}^s = \mathcal{C} \quad (2.5.13)$$

$$\nabla^4 \psi^s = \frac{g}{\eta} \frac{\partial \rho}{\partial x} \quad (2.5.14)$$

Now doesn't that make you feel much better. What is less than obvious is that Eqs. (2.5.11)–(2.5.13) form a non-linear wave equation for porosity while Eq. (2.5.14) governs rotational flow (convection) due to lateral density gradients. These equations are similar to those of infinite prandtl number thermal convection however, now the principal source of buoyancy is the presence of a low density melt (i.e. the porosity) which does *not* behave like temperature.

### Scaling

Equations (2.5.11)–(2.5.14) may appear to contain a large number of parameters, however, as is often the case, a judicious choice of scaling removes most of them. If we define a characteristic porosity  $\phi_0$  (say 0.01), then we can define a naturally occurring length scale, *the compaction length*

$$\delta = \sqrt{\frac{k_0(\zeta + 4\eta/3)}{\mu}} \quad (2.5.15)$$

which depends on  $k_0$ , the permeability at porosity  $\phi_0$ , and the ratio of solid and liquid viscosities. We can also define the natural velocity scale *the separation velocity*

$$w_0 = \frac{k_0 \Delta \rho g}{\mu} \quad (2.5.16)$$

which is velocity the melt would move *relative* to the solid if it were driven solely by gravity in a porous medium with constant permeability  $k_\phi(\phi_0)$ . With these two definitions, we can form the following scaling

$$\phi = \phi_0 \phi'$$

$$\begin{aligned}
\mathbf{x} &= \delta \mathbf{x}' \\
t &= (\delta/w_0)t' \\
\mathcal{C} &= (\phi_0 w_0 / \delta) \mathcal{C}' \\
\Gamma &= (\rho_s \phi_0 w_0 / \delta) \Gamma' \\
\mathcal{U} &= (\phi_0 w_0 \delta) \mathcal{U}' \\
\psi &= (w_0 \delta) \psi' \\
k_\phi &= k_0 k'_\phi
\end{aligned} \tag{2.5.17}$$

$$\tag{2.5.18}$$

Substituting and dropping primes as usual yields the following dimensionless equations

$$\frac{\partial \phi}{\partial t} + \mathbf{V} \cdot \nabla \phi = (1 - \phi_0 \phi) \mathcal{C} + \Gamma \tag{2.5.19}$$

$$-\nabla \cdot k_\phi \nabla \mathcal{C} + \mathcal{C} = \nabla \cdot k_\phi \left[ \frac{\nu}{\phi_0} \nabla \times \nabla^2 \psi^s \mathbf{j} - (1 - \phi_0 \phi) \mathbf{k} \right] + \Gamma \Delta v \tag{2.5.20}$$

$$\nabla^2 \mathcal{U}^s = \mathcal{C} \tag{2.5.21}$$

$$\nabla^4 \psi^s = \frac{\phi_0}{\nu} \frac{\partial \phi}{\partial x} \tag{2.5.22}$$

where  $\nu = \eta / (\zeta + 4\eta/3)$ . See [13, 14] for further details.

### Some solutions

These equations contain a surprising amount of behaviour that arises simply from the physical requirements that the solid medium is permeable and deformable. This behaviour ranges from the development of non-linear porosity waves in 1,2 and 3 dimensions [10, 11, 13–17], porous media convection [18, 19], and applications to mid-ocean ridges and island arcs [20–28]. In particular, these equations have been instrumental in understanding the observable geochemical consequences of magma transport and have shown that by including explicit melt and solid transport into equations of chemical transport (next section), surprising and new inferences may be drawn from available data [22, 29–34]. Figure 2.8 shows a rogues gallery of solutions (without much explanation) of some of these problems.

## 2.6 Geochemical Transport/Reactive flows

Finally, the last class of general problems that we will discuss (briefly) in this chapter is the transport and interaction of chemical species in multi-phase flows. Given the equations for general conservation of mass and momentum for coupled fluid solid flows, it is easy to write down conservation equations for the mass of individual chemical constituents. A general form for component  $i$  that is conserved in both the liquid and solid phases can be written

$$\frac{\partial \rho_f \phi c_i^f}{\partial t} + \nabla \cdot [\rho_f \phi c_i^f \mathbf{v}] = \nabla \cdot \phi D_i^f \nabla c_i^f + \sum_{j=1}^J c_{ij}^{f*} \Gamma_j \tag{2.6.1}$$

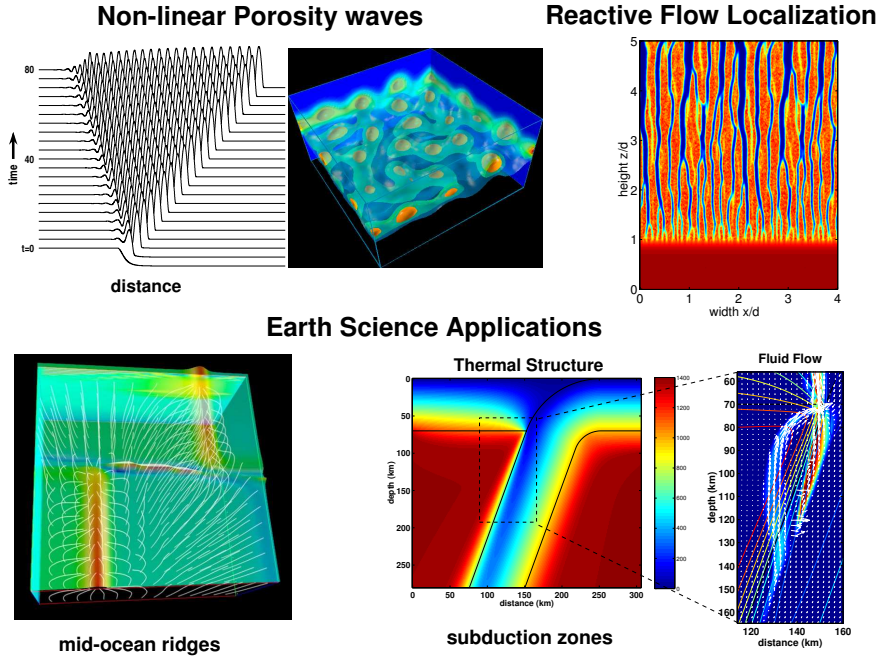


Figure 2.8: A rogues gallery of solutions for flow in deformable porous media

$$\frac{\partial \rho_s (1 - \phi) c_i^s}{\partial t} + \nabla \cdot [\rho_s (1 - \phi) c_i^s \mathbf{V}] = - \sum_{j=1}^J c_{ij}^{f*} \Gamma_j \quad (2.6.2)$$

where  $c_i^f$ ,  $c_i^s$  are the concentration of component  $i$  in the melt and solid respectively.  $\mathcal{D}_i^f$  is the diffusivity (or dispersivity) of component  $i$  in the melt (we assume negligible solid diffusion) and  $c_{ij}^{f*}$  is the concentration of component  $i$  in the fluid that is produced by reaction  $j$ .  $\Gamma_j$  is just the rate of mass transfer for reaction  $j$ . To make Eqs. (2.6.1)–(2.6.2) consistent with Eqs. (2.5.4)–(2.5.5) and the property that the sum of all concentrations in any phase must add to 100% (e.g.  $\sum_{i=1}^N c_i^f = \sum_{i=1}^N c_i^s = \sum_{i=1}^N c_{ij}^{f*} = 1$ ) requires that the total mass transfer rate be

$$\Gamma = \sum_{j=1}^J \Gamma_j \quad (2.6.3)$$

and that  $\sum_{i=1}^N \nabla \cdot \phi \mathcal{D}_i^f \nabla c_i^f = 0$  because only  $N - 1$  concentrations can freely diffuse. The final component must be anti-diffusive to conserve mass. For extensions to more complicated multi-phase systems see [35]. When these equations are coupled to the equations of motions in reactive systems, significant flow localization can occur due to reactive feed back between fluid flow and dissolution [36–39].

## Bibliography

- [1] J. Gleick. *Chaos*, Penguin, 1987, Q172.5.C45G54.
- [2] E. N. Lorenz. Deterministic non-periodic flow, *J. Atmos. Sci.* 20, 130, 1963.
- [3] A. E. Gill. *Atmosphere-ocean dynamics*, International geophysics series, Academic Press, New York, 1982.
- [4] J. Y. K. Cho and L. M. Polvani. The morphogenesis of bands and zonal winds in the atmospheres on the giant outer planets, *Science* 273, 335–337, Jul 1996.
- [5] S. E. Zebiak. Tropical atmosphere-ocean interaction and the El Niño/Southern Oscillation phenomenon, Ph.D. thesis, Massachusetts Institute of Technology, Cambridge, MA, 1985.
- [6] M. A. Cane, S. E. Zebiak and S. C. Dolan. Experimental forecasts of el nino, *Nature* 321, 827–832, 1986.
- [7] S. E. Zebiak and M. A. Cane. A model el niño-southern oscillation, *Mon. Wea. Rev.* 115, 2262–2278., 1987.
- [8] G. Dagan. *Flow and Transport in Porous Formations*, Springer-Verlag, Berlin, 1989.
- [9] D. McKenzie. The generation and compaction of partially molten rock, *J. Petrol.* 25, 713–765, 1984.
- [10] D. R. Scott and D. Stevenson. Magma solitons, *Geophys. Res. Lett.* 11, 1161–1164, 1984.
- [11] D. R. Scott and D. Stevenson. Magma ascent by porous flow, *J. Geophys. Res.* 91, 9283–9296, 1986.
- [12] A. C. Fowler. A mathematical model of magma transport in the asthenosphere, *Geophys. Astrophys. Fluid Dyn.* 33, 63–96, 1985.
- [13] M. Spiegelman. Flow in deformable porous media. part 1. Simple analysis, *J. Fluid Mech.* 247, 17–38, 1993.
- [14] M. Spiegelman. Flow in deformable porous media. part 2. Numerical analysis—The relationship between shock waves and solitary waves, *J. Fluid Mech.* 247, 39–63, 1993.
- [15] V. Barcilon and O. Lovera. Solitary waves in magma dynamics, *J. Fluid Mech.* 204, 121–133, 1989.
- [16] V. Barcilon and F. M. Richter. Non-linear waves in compacting media, *J. Fluid Mech.* 164, 429–448, 1986.

- [17] C. Wiggins and M. Spiegelman. Magma migration and magmatic solitary waves in 3-D, *Geophys. Res. Lett.* 22, 1289–1292, May 15 1995.
- [18] D. R. Scott. The competition between percolation and circulation in a deformable porous medium, *J. Geophys. Res.* 93, 6451–6462, 1988.
- [19] D. R. Scott and D. J. Stevenson. A self-consistent model of melting, magma migration and buoyancy-driven circulation beneath mid-ocean ridges, *J. Geophys. Res.* 94, 2973–2988, 1989.
- [20] M. Spiegelman and D. McKenzie. Simple 2-D models for melt extraction at mid-ocean ridges and island arcs, *Earth Planet. Sci. Lett.* 83, 137–152, 1987.
- [21] M. Spiegelman. Physics of melt extraction: Theory, implications and applications, *Philos. Trans. R. Soc. London, Ser. A* 342, 23–41, 1993.
- [22] M. Spiegelman. Geochemical consequences of melt transport in 2-D: The sensitivity of trace elements to mantle dynamics, *Earth Planet. Sci. Lett.* 139, 115–132, 1996.
- [23] D. R. Scott. Small-scale convection and mantle melting beneath mid-ocean ridges, in: J. Phipps Morgan, D. K. Blackman and J. M. Sinton, eds., *Mantle flow and melt generation at mid-ocean ridges*, vol. 71 of *Geophysical Monograph*, pp. 327–352, Amer. Geophys. Union, 1992.
- [24] D. W. Sparks and E. M. Parmentier. Melt extraction from the mantle beneath spreading centers, *Earth Planet. Sci. Lett.* 105, 368–377, 1991.
- [25] D. W. Sparks, E. M. Parmentier and J. P. Morgan. Three-dimensional mantle convection beneath a segmented spreading center: Implications for along-axis variations in crustal thickness and gravity, *J. Geophys. Res.* 98, 21977–21995, Dec 1993.
- [26] D. W. Sparks and E. M. Parmentier. The structure of three-dimensional convection beneath oceanic spreading centres, *Geophys. J. Int.* 112, 81–91, Jan. 1993.
- [27] L. Magde and D. W. Sparks. Three-dimensional mantle upwelling, melt generation and melt migration beneath segmented slow-spreading ridges, *J. Geophys. Res.* 102, 20571–20583, 1997.
- [28] K. Barnouin-Jha, E. M. Parmentier and D. W. Sparks. Buoyant mantle upwelling and crustal production at oceanic spreading centers: On-axis segmentation and off-axis melting, *J. Geophys. Res.* 102, 11979–11989, 1997.
- [29] S. Watson and M. Spiegelman. Geochemical effects of magmatic solitary waves, *Geophys. J. Int.* 117, 284–295, 1994.
- [30] M. Spiegelman. Geochemical effects of magmatic solitary waves: some analysis, *Geophys. J. Int.* 117, 296–300, 1994.

- [31] M. Spiegelman and T. Elliott. Consequences of melt transport for U-series disequilibrium in young lavas, *Earth Planet. Sci. Lett.* 118, 1–20, 1993.
- [32] M. Spiegelman and J. Reynolds. Combined theoretical and observational evidence for convergent melt flow beneath the EPR, *Nature* 402, 282–285, Nov. 1999.
- [33] M. Spiegelman. UserCalc: a web-based U-series calculator for mantle melting problems, *Geochem. Geophys. Geosyst.* 1, 2000, Paper Number 1999GC000030.
- [34] M. Spiegelman and P. B. Kelemen. Extreme chemical variability as a consequence of channelized melt transport, for submission to *Science*.
- [35] C. I. Steefel and A. C. Lasaga. A coupled model for transport of multiple chemical species and kinetic precipitation/dissolution reactions, *Am. J. Sci.* 294, 529–592, 1994.
- [36] P. B. Kelemen, J. A. Whitehead, E. Aharonov and K. A. Jordahl. Experiments on flow focusing in soluble porous media, with applications to melt extraction from the mantle., *J. Geophys. Res.* 100, 475, Jan 1995.
- [37] E. Aharonov, J. Whitehead, P. B. Kelemen and M. Spiegelman. Channeling instability of upwelling melt in the mantle, *J. Geophys. Res.* 100, 20433–20450, 1995.
- [38] E. Aharonov, M. Spiegelman and P. B. Kelemen. Three-dimensional flow and reaction in porous media: Implications for the Earth's mantle and sedimentary basins, *J. Geophys. Res.* 102, 14821–14834, 1997.
- [39] M. Spiegelman, P. B. Kelemen and E. Aharonov. Causes and consequences of flow organization during melt transport: The reaction infiltration instability in compactible media, *J. Geophys. Res.* 106, 2061–2077, 2001, [www.ldeo.columbia.edu/~mspieg/SolFlow/](http://www.ldeo.columbia.edu/~mspieg/SolFlow/).